

Journal of Materials Chemistry C

Accepted Manuscript



This is an *Accepted Manuscript*, which has been through the Royal Society of Chemistry peer review process and has been accepted for publication.

Accepted Manuscripts are published online shortly after acceptance, before technical editing, formatting and proof reading. Using this free service, authors can make their results available to the community, in citable form, before we publish the edited article. We will replace this *Accepted Manuscript* with the edited and formatted *Advance Article* as soon as it is available.

You can find more information about *Accepted Manuscripts* in the [Information for Authors](#).

Please note that technical editing may introduce minor changes to the text and/or graphics, which may alter content. The journal's standard [Terms & Conditions](#) and the [Ethical guidelines](#) still apply. In no event shall the Royal Society of Chemistry be held responsible for any errors or omissions in this *Accepted Manuscript* or any consequences arising from the use of any information it contains.

Cite this: DOI: 10.1039/c0xx00000x

www.rsc.org/xxxxxx

ARTICLE TYPE

Intrinsic Low Dielectric Behaviour of a Highly Thermal Stable Sr-Based Metal–Organic Framework for Interlayer Dielectric Materials

Muhammad Usman,^{a,b,c} Cheng-Hua Lee,^a Dung-Shing Hung,^d Shang-Fan Lee,^e Chih-Chieh Wang,^f Tzuoo-Tsair Luo,^a Zhao Li,^e Mau-Kuen Wu,^e Kuang-Lieh Lu^{*a}

5 Received (in XXX, XXX) Xth XXXXXXXXXX 20XX, Accepted Xth XXXXXXXXXX 20XX

DOI: 10.1039/b000000x

A Sr-based metal–organic framework $\{[\text{Sr}_2(1,3\text{-bdc})_2(\text{H}_2\text{O})_2] \cdot \text{H}_2\text{O}\}_n$ (**1**) was synthesized under hydrothermal conditions by the reaction of $\text{Sr}(\text{NO}_3)_2$ and 1,3-bis-(4,5-dihydro-2-oxazolyl)benzene. A single-crystal X-ray diffraction analysis revealed that compound **1** adopts a 2D layer structure with a monoclinic (*C2/c*) space group. The distance between the layers of the structure adjust, upon the removal of the water molecules from 95 °C to 330 °C. In addition, the dehydrated compound **1'** retains its crystalline morphology and shows a high thermal stability at temperatures of up to 420 °C. Significantly, the dehydrated compound **1'** has a very low dielectric constant (2.4), suggesting that it might be useful as an interlayer dielectric in integrated circuits. As indicated by impedance spectroscopy, such low dielectric constant behavior is due to the intrinsic nature of the bulk material. The preparation of a low dielectric constant of Sr-based metal–organic framework with a high thermal stability opens new directions for research in their applications.

1. Introduction

The design and synthesis of low dielectric constant (low-k) materials has been a subject of interest in terms of their potential for use in high performance electronics devices. With continuous shrinking dimensions and the increasing number of active devices with integrated circuits (ICs), interconnect resistive-capacitive (*RC*) delay and electronics cross-talk becomes a major issue and pose serious limitations on device performance.¹ For faster and higher performance microelectronics devices, a low-k material for replacing silicon dioxide (SiO_2) as a interlayer dielectric is needed.² According to the international technology roadmap for semiconductors, porous materials and air gap structures will take the place of low-k materials for interlayer dielectrics in multilevel interconnect schemes in the near future, thus substantially reducing the interconnect *RC* delay and electronics crosstalk in ICs.³ Some recent reports have appeared dealing with the preparation of porous silica-based materials,⁴⁻⁶ fluorinated amorphous carbon,⁷ benzoxazine-based polymers,⁸⁻¹⁰ and organometallic compounds¹¹ for use as low-k materials as interlayer dielectrics. However, there are number of requirements for the new low-k materials, including a thermal stability at temperatures of 400 °C or higher, electrically insulating, high mechanical strength, and good adhesion to neighboring layers.^{1,12}

Metal–organic frameworks (MOFs)¹³⁻¹⁶ with a highly uniform porosity, large surface area, ultralow densities, high stability and easy tunability of the surface and structural properties have potential for use as stable low-k materials.¹⁷⁻²⁰ MOFs have been extensively studied over the past decade for their applications in gas storage,²¹⁻²⁵ sensing,²⁶ chemical separation,^{27,28} catalysis,²⁹⁻³²

drug delivery and biomedical imaging.^{33,34} Following the roadmap for implementation of MOFs in electronics devices by Allendorf and Talin,³⁵ some reports have been appeared on the magnetic,³⁶⁻³⁸ optical^{39,40} and ferroelectric^{41,42} behaviour of MOFs. Recently, an article discussing the dielectric bistability of a strontium-based MOF was reported.⁴³ Hermann and co-workers presented a theoretical model for using MOFs as low-k materials in future applications.⁴⁴ While to date, there is only one recent experimental example of the possible use of ZIF-8 films as low-k materials for an inter-layer dielectric in microelectronic chip devices. ZIF-8 has a low dielectric constant of only 2.33 (± 0.05) at 100 kHz with a thermal stability of 350 °C.⁴⁵ In order to identify new low-k materials with good thermal stability, we are currently working to develop porous materials having strong bonding that cannot decompose easily at high temperature. In this work, we report on the preparation of a unique strontium-based MOF $\{[\text{Sr}_2(1,3\text{-bdc})_2(\text{H}_2\text{O})_2] \cdot \text{H}_2\text{O}\}_n$ (**1**) along with an unusually high thermal stability and a low dielectric constant of its dehydrated sample **1'**. The dehydrated compound **1'** possesses a very low dielectric constant (2.4) with high thermal stability at temperatures up to 420 °C, making it a potential candidate for use as an interlayer dielectric in ICs. To the best of our knowledge, this work is the first example of highly stable Sr-based metal–organic framework with the potential for use as a low dielectric material as interlayer dielectric in microelectronics devices.

2. Experimental Section

2.1 Materials and Instruments

Chemical reagents were purchased commercially and were used

as received without further purification. Diffraction measurements for compound **1** were carried out using a Bruker-Nonius Kappa CCD diffractometer with graphite-monochromated Mo K α radiation ($\lambda = 0.7107 \text{ \AA}$). Data collection parameters of compound **1** are listed in Table S1 (See Supplementary Information). Structure was solved using direct methods and refined using the SHELXL-97 program by full-matrix least-squares on F^2 values. All non-hydrogen atoms were refined anisotropically, whereas the hydrogen atoms were placed in ideal, calculated positions, with isotropic thermal parameters riding on their respective carbon atoms. Elemental analyses were conducted on a Perkin-Elmer 2400 CHN elemental analyzer. Thermogravimetric (TG) analyses were performed under nitrogen with a Perkin-Elmer TGA-7 TG analyzer. The temperature-dependent X-ray powder diffraction experiments were performed at the beam line BL01C2 of the National Synchrotron Radiation Research Centre (NSRRC) of Taiwan. The radiation was generated from the superconducting wavelength shifter magnet of 5.0 Tesla with ring energy of 1.5 GeV and ring current of 360 mA under top-up mode operation. The wavelength of incident X-ray was 1.03321 \AA which delivered by a Si(111) double crystal monochromator. The powder sample was packed in a quartz capillary of 1.0 mm diameter and the *in-situ* temperature dependent experiment was heated in a stream of hot air from room temperature to 450 $^\circ\text{C}$ with a heating rate approximately 10 $^\circ\text{C}/\text{min}$. Two dimensional powder diffraction patterns were recorded by a Mar345 imaging plate detector with the pixel size of 100 μm and the exposure time of each images were 72 seconds. The sample to imaging plate distance was 302.77 mm and the diffraction angle was calibrated according to Bragg positions of Ag-Behenate and Si (NBS640b) standards. The one dimensional XRD profile was converted using the FIT2D program of a cake type integration.

2.2 Synthesis of $\{[\text{Sr}_2(1,3\text{-bdc})_2(\text{H}_2\text{O})_2] \cdot \text{H}_2\text{O}\}_n$ (**1**)

Compound $\{[\text{Sr}_2(1,3\text{-bdc})_2(\text{H}_2\text{O})_2] \cdot \text{H}_2\text{O}\}_n$ (**1**) was synthesized through a self assembly process by reacting $\text{Sr}(\text{NO}_3)_2$ (0.0212 g, 0.1 mmol) and 1,3-bis-(4,5-dihydro-2-oxazolyl)benzene (0.0216 g, 0.1 mmol) in a EtOH-H $_2\text{O}$ (3 mL:1 mL) solution under hydrothermal conditions at 180 $^\circ\text{C}$ for 72 h followed by allowing the solution to slowly cooled at a rate of 3.1 $^\circ\text{C}/\text{h}$. The colorless square crystals of **1**, suitable for single-crystal X-ray diffraction were filtered by washing the crystals with water, and dry at ambient temperature. Yield: 23.9% (13.3 mg; 0.02 mmol). Anal. Calcd for $\text{C}_{16}\text{H}_{14}\text{O}_{11}\text{Sr}_2$: C, 34.47; H, 2.53. Found: C, 34.37; H, 2.83.

2.3 Electrical Characterization Techniques

Complex dielectric measurements were carried out with an Agilent 4294A network analyzer connected to an Agilent 16451B dielectric test fixture over a frequency range of 40 Hz to 0.1 MHz at room temperature. Pellets of compound **1** having water molecules and dehydrated compound **1'** were prepared from a powdered sample through high pressure (30 MPa). A contact electrode method was used with 5 mm guarded/unguarded electrodes. The capacitance (Cp) and dielectric loss (D) were directly recorded from the network analyzer. The dielectric constant was determined by equation 1:

$$K = \text{Cpd}/\epsilon_0 A \quad (1)$$

Here, ϵ_0 is the dielectric permittivity in a vacuum ($8.85 \times 10^{-12} \text{ F/m}$); A is the area of the electrode (m^2), and d is the thickness of the film (m). Impedance spectrum fitting results are plotted using Zview software program. Electrical characterizations have been performed using electrochemical workstation (AUTOLAB PGST30, Eco Chemie).

3. Result and Discussion

3.1 Synthesis of Compound 1

Strontium-based materials have recently become widely use in the semiconductor industry because of their thermal stability, high reactivity and good mechanical strength.^{46,47} However, there are very few reports on strontium-based MOFs. In this study, compound $\{[\text{Sr}_2(1,3\text{-bdc})_2(\text{H}_2\text{O})_2] \cdot \text{H}_2\text{O}\}_n$ (**1**) was synthesized by reacting $\text{Sr}(\text{NO}_3)_2$ and 1,3-bis-(4,5-dihydro-2-oxazolyl)benzene in an EtOH-H $_2\text{O}$ solution under hydrothermal conditions at 180 $^\circ\text{C}$ for 3 days (Figure 1). Compound **1** was obtained as colorless square crystals. FTIR data are shown in Figure S1 (see Supplementary Information). The crystal data of **1** are shown in Table S1 (see Supplementary Information) and temperature dependent powder X-ray pattern is shown in Figure 5. It is noteworthy that the 1,3-bis-(4,5-dihydro-2-oxazolyl)benzene ligand is degraded during the hydrothermal synthesis, giving rise to the 1,3-bdc ligand present in the title compound. A similar reaction, carried out by directly using the 1,3-dicarboxylic acid as ligand, afforded compound **1** in a yield of 17.2%.

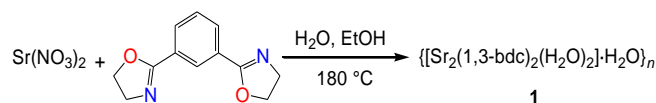


Fig. 1 Synthesis of compound **1**.

3.2 Crystal Structure

A single-crystal X-ray diffraction analysis showed that **1** displays a 2D structure and crystallizes in the monoclinic $C2/c$ space group.⁴⁸ The asymmetric unit consists of two strontium ions, two 1,3-btc ligands and two coordinated water molecules as well as a free H $_2\text{O}$ molecule. The Sr(III) ions have two coordination modes. The Sr(1) atom adopts a seven-coordinated geometry by six oxygen atoms ($\text{O}_1, \text{O}_3, \text{O}_5, \text{O}_6, \text{O}_7, \text{O}_8$) of five carboxylic groups from five 1,3-btc ligands and one oxygen atom (O_9) from the coordinated H $_2\text{O}$ molecule as shown in Figure S3(a) (See Supplementary Information). With SrO $_8$ coordination geometry shown in Figure S3(b) (See Supplementary Information), the Sr(2) atom is eight-coordinated by seven oxygen atoms ($\text{O}_1, \text{O}_2, \text{O}_3, \text{O}_4, \text{O}_6, \text{O}_7, \text{O}_8$) of five carboxylate groups from five 1,3-btc ligands and one oxygen atom (O_{10}) from coordinated H $_2\text{O}$. Each 1,3-btc ligand acts as a μ_5 -bridge to link five Sr atoms. The carboxylate groups adopt $\mu_2\text{-}\eta^2\text{-}\eta^1$ -bridging, and $\mu_3\text{-}\eta^2\text{-}\eta^2$ -bridging coordination modes. As shown in Figure 2, the carboxylate groups and Sr(III) ions constructed $[\text{Sr}_4(\text{COO})_8]$ units, which

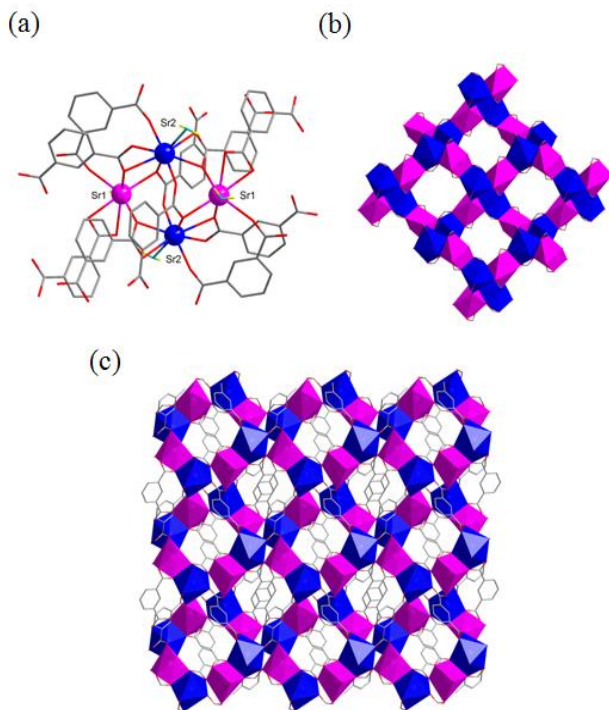


Fig. 2 (a) The $\text{Sr}_4(\text{COO})_8$ metal cluster of **1** (b) 2D layer of **1** constructed through Sr-metal clusters (c) 2D framework of **1** along the a -axis.

form 2D layers. The 2D layer structure has strong hydrogen bonds that serve to enhance net-to-net interactions (Figure 3). The guest H_2O molecules are stabilized between two layers by (O–H \cdots O) hydrogen bonding interaction (O11 \cdots O7 = 1.89 Å; O11 \cdots O7 = 1.87 Å). To remove H_2O molecules, compound **1** was treated at high temperature under a vacuum. The surface morphology of the dehydrated compound **1'** does not change substantially as the result of dehydration process, as shown in Figure S4 (See Supplementary Information). However, the crystal transparency decreases after the water molecules are removed.

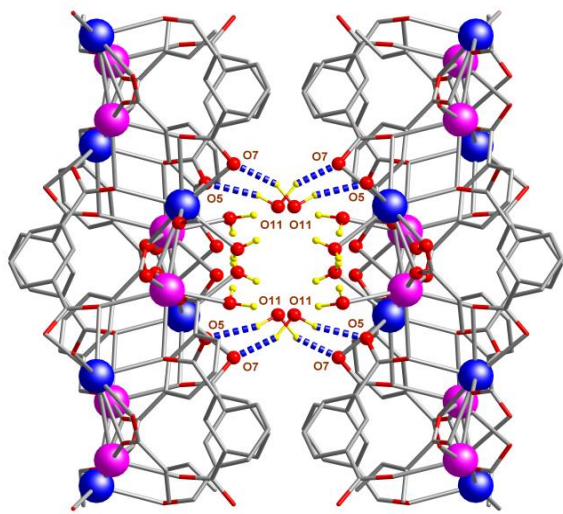


Fig. 3 The host-guest hydrogen bonding interactions of **1**.

3.3 Thermal Stability

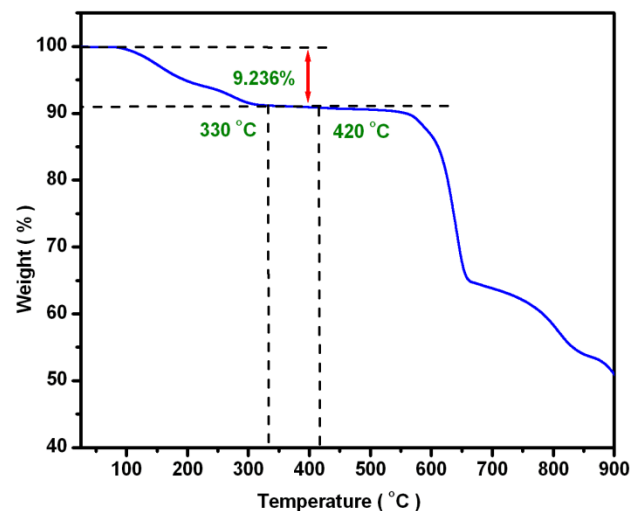


Fig. 4 Thermogravimetric (TG) diagram for compound **1**

A thermogravimetric (TG) analysis of **1** (Figure 4) showed that the coordinated and guest water molecules are released at temperatures between 95 °C and 330 °C (Experimental: 9.4%, calculated: 10.3%). In the temperature range of approximate 330 °C–420 °C, the dehydrated sample **1'** was stable without any weight loss. The thermal stability of the materials was further investigated by *in-situ* powder X-ray diffractometry, as shown in Figure 5. The powder pattern of a fresh sample at 50 °C essentially matches the simulated pattern based on the single crystal structure. The powder patterns are nearly constant, in the temperature range from 50 to 330 °C and a phase transition is observed at 360 °C. The peak ($2\theta \approx 5.75^\circ$) for the (200) plane shows an obvious shift after the H_2O molecules are removed, as shown in Figure 5. The 2D metal-organic skeleton of **1** grows along the bc plane and the layers are packed with guest molecules along the a axis. Therefore, the distance between the layers may shrink and the peak for the (200) plane shifts to a higher angle. From 360 °C to 420 °C, the PXRD patterns are all similar, indicating the existence of a dehydrated form (**1'**) of **1**. While the

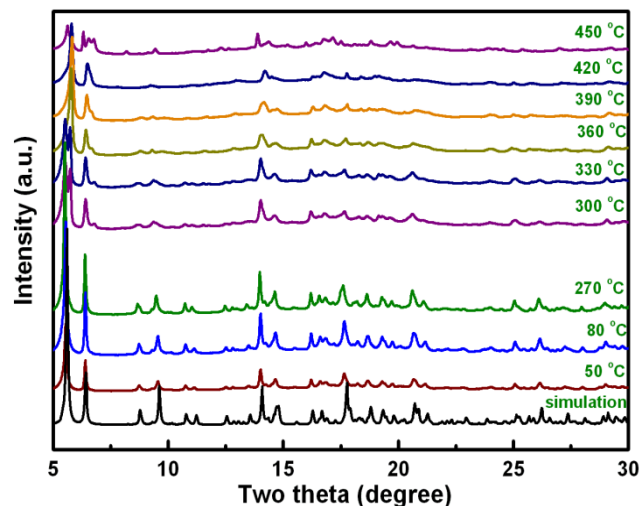


Fig. 5 Simulated and temperature-dependent experimental powder X-ray diffraction patterns of compound **1**.

decomposition process has started at 450 °C. This result is consistent with the TGA data. Having a high thermal stability, makes **1'** a suitable candidate to use as an interlayer dielectric material.^{7,12}

3.4 Dielectric Properties

A temperature dependent dielectric study from 0 to 350 K was carried out, as shown in Figure 6. As the compound **1** is heated from 0 to 350 K, the dielectric constant (k) increases, indicating the motion of water molecules due to freezing and defreezing.^{49,50} To get low dielectric material, water was completely removed from **1**. The frequency dependence for the permittivity [$\epsilon'_r(\omega) + \epsilon''_r(\omega)$] of compound **1** and the dehydrated sample **1'** was measured at room temperature, in which $\epsilon'_r(\omega)$ (dielectric constant) and $\epsilon''_r(\omega)$ (dielectric loss) are the respective real and imaginary parts of the permittivity. From Figure 7, it can be seen that the value of the relative permittivity (ϵ'_r) of **1** reached its highest value at a very low frequency and then rapidly decreased to 7.31 with increasing frequency. After removing the H₂O molecules, the value of the dielectric constant of the dehydrated sample **1'** decreases significantly to a low value of 2.40 at a low frequency. The presence of the polar water molecules between the layers at low frequency is the reason for the relatively high value (23 at 1 kHz) of the dielectric constant of **1**. Because the mobility of the dipole of **1** decreases at higher frequencies, the dipole polarization would also be expected to decrease. For this reason, the dielectric constant (k) shows decaying behavior with an increase in frequency for compound **1**. On the other hand, after removing the polar H₂O molecules, the dipole polarization due to water molecules in the dehydrated sample **1'** will be absent, therefore, a low dielectric value of 2.4 at 1 MHz with a very low dielectric loss (0.026) was observed. After removing the H₂O molecules, for compound **1'**, the dipole moment is already less, even at low frequencies. As a result, no decay was observed for the compound when H₂O molecules were absent.^{49,50}

Dielectric loss follows the same decaying trend with increasing frequency (0.45 to 0.28) for compound **1** as shown in Figure S5 (See Supporting Information). While after removing the H₂O molecules, the dielectric loss for compound **1'** decreased to

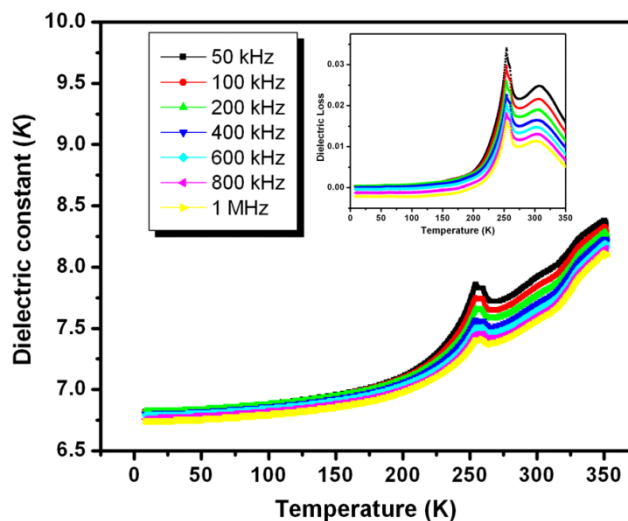


Fig. 6 Temperature dependent dielectric constants from 0 to 350 K at different frequencies for compound **1** with dielectric loss in the offset.

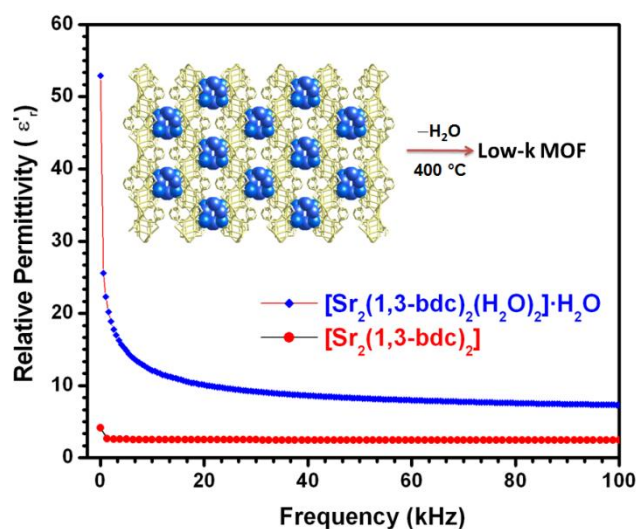


Fig. 7 Relative permittivity vs frequency for **1** and dehydrated sample **1'** at room temperature.

0.0159. The dielectric loss is due to various polarization processes, series resistance and the capacitance of the electrodes.^{51,52} Such decaying behavior of a dielectric constant (k) at low frequency has also been reported for perovskite-related oxide CaCu₃Ti₄O₁₂,⁵³ Q[8](CuCl₂)_{0.75}·30(H₂O) (Q[8] = Cucurbit[8]-uril),⁵⁴ (CBQ)CuI₃(CN)₃Br,⁵⁵ homochiral zinc-quitenine coordination polymer,⁵² ZIF-8 films⁴⁵ and [(Mn₃(HCOO)₆)(H₂O)(CH₃OH)].⁴⁹

3.5 Impedance spectroscopy

To further investigate the dielectric behavior of compound **1'**, we carried out impedance spectroscopy studies (Z' Vs Z'') as a function of frequency at room temperature. The impedance curves can be fitted by the equivalent circuit using the Zview fitting program. Experimental and simulated results indicate that the low dielectric constant is due to the intrinsic behavior of **1'**. The single large arc can be modeled by two equivalent circuits connected in series with each other. First circuit contains two elements connected in parallel: a resistance (R_1) and a capacitance phase element (CPE1), which indicates the impedance of the bulk material. The second circuit contains a resistance (R_2) in parallel with a capacitance phase element (CPE2) representing the impedance for the interface between the electrodes and bulk material. The impedance curves in Figure 8(a) and 8(b) intercept zero at room temperature and the order of magnitude of their capacitance is pF cm⁻¹ which is due to the intrinsic behavior of the material bulk. There is only one contribution, so the low dielectric response of compound **1'** is purely intrinsic at room temperature.⁵⁶⁻⁵⁸ Ionic conductivity can be calculated using the equation $\sigma = d/RA$ where d is the thickness of the bulk material and R is the resistance determined from the impedance fitting curves for an equivalent circuit and A is the area of the electrode. From the above results in Figure 8 and Figure 9, the value of R_1 for compound **1** and dehydrated sample **1'** was calculated to be $1.13 \times 10^5 \Omega$ and $8.83 \times 10^7 \Omega$, respectively. From these values for the resistance, the ionic conductivity for compound **1** with H₂O molecules is calculated to be 6.56×10^{-6} S/cm, which is significantly higher than that for

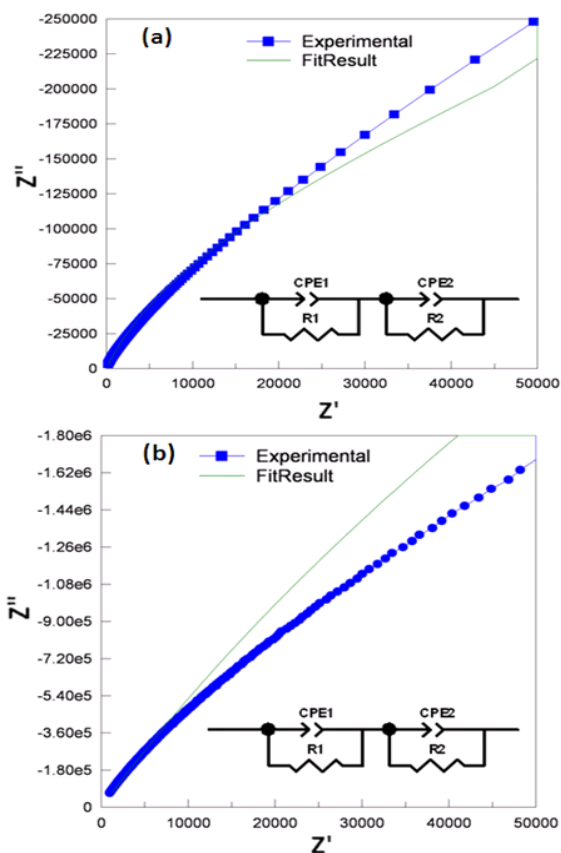


Fig. 8 Impedance spectroscopy with the equivalent circuits for (a) compound **1** with H₂O molecules and (b) dehydrated product **1'**.

dehydrated product **1'** with an ionic conductivity of 4.96×10^{-9} S/cm. The dehydrated compound **1'** has much low ionic conductivity than compound **1** itself, which justifies the lower value of dielectric constant of dehydrated sample **1'** than compound **1**. Such a low value for ionic conductivity indicates that the dehydrated product **1'** has the insulating characteristics which is required for low-*k* materials.⁴⁵

3.6 Leakage current characteristics

To assess the quality of the dielectric, we measured leakage

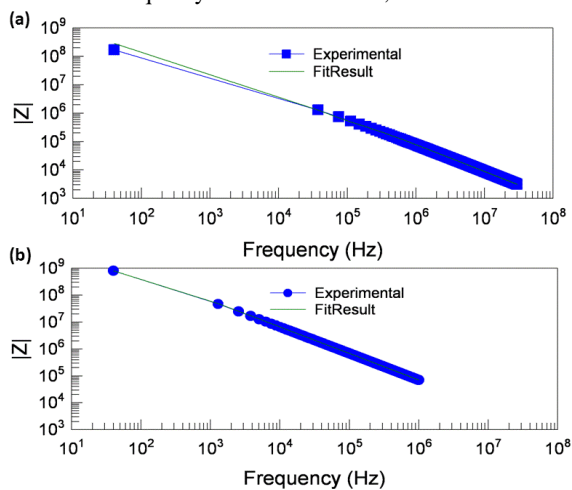


Fig. 9 Impedance vs frequency experimental and fitted results are shown for (a) compound **1**, and (b) dehydrated compound **1'**.

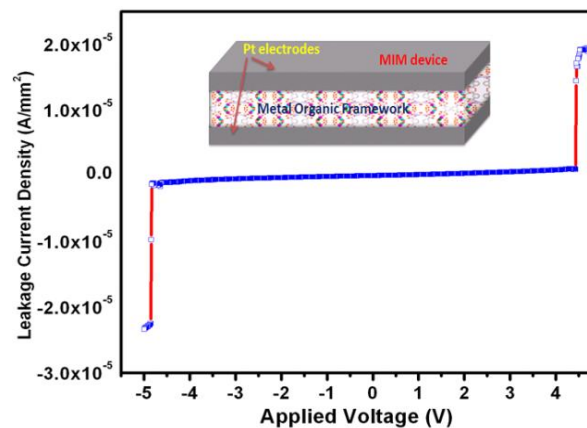


Fig. 10 Plot of leakage current (*I*) versus applied voltage (*V*) of the dehydrated sample **1'** prepared as MIM device using platinum electrodes.

current as a function of voltage in a MIM capacitor configuration and the results are shown in Figure 10. Platinum (Pt) electrodes of 30 nm thickness were coated on the pellet of the dehydrated compound **1'** (250 nm) to make MIM device. A low leakage current of 1.69×10^{-9} A/mm² with a breakdown voltage of -4.9 V is observed at ambient conditions.

4. Conclusions

We report herein on the synthesis, structure, and dielectric properties of a novel Sr-based metal–organic framework $\{[\text{Sr}_2(1,3\text{-bdc})_2(\text{H}_2\text{O})_2] \cdot \text{H}_2\text{O}\}_n$. Data obtained from a thermogravimetric (TG) analysis revealed that the dehydrated product **1'** is highly thermally stable at temperatures of up to 420 °C. After removing the H₂O molecules, the dehydrated compound **1'** has a low dielectric constant (2.4) at room temperature. Such low dielectric behaviour is due to the intrinsic property of the bulk material, as evidenced by impedance measurements. A low dielectric constant and high thermal stability make this Sr-based MOF a candidate for use as a low-*k* material for potential interlayer dielectric applications. The foregoing results discussed in this work will provide an effective path towards remarkable new applications of stable MOFs as interlayer dielectrics in the future.

Acknowledgements

We gratefully acknowledge Academia Sinica, Taiwan for their financial support for PhD program through a platform of Taiwan International Graduate Program (TIGP). We also thank to National Science Council (NSC), Taiwan for their financial support.

Notes and references

- ^aInstitute of Chemistry, Academia Sinica, Taipei 115, Taiwan
⁴⁰E-mail: kllu@gate.sinica.edu.tw, Fax: +886-2-27831237
^bDepartment of Physics, National Central University, Chung-Li 320, Taiwan
^cInstitute of Atomic and Molecular Science, Academia Sinica, Taipei 106, Taiwan
⁴⁵^dDepartment of Information and Telecommunications Engineering, Ming Chuan University, Taipei 111, Taiwan

^aInstitute of Physics, Academia Sinica, Taipei 115, Taiwan

^fDepartment of Chemistry, Soochow University, Taipei 100, Taiwan

†Electronic Supplementary Information (ESI) available: [Crystallographic data (CIF), Crystal and structure refinement data (Table S1); IR spectra of ligands and compound **1** (Figure S1); Orientation of water molecules in framework (Figure S2); Coordination modes for Sr (Figure S3); Surface morphology of single crystal (Figure S4); Dielectric Loss vs frequency (Figure S5); Leakage current (Figure S6). See DOI: 10.1039/b000000x/

1. W. Volksen, R. D. Miller and G. Dubois, *Chem. Rev.*, 2010, **110**, 56.
2. S. J. Martin, J. P. Godschalx, M. E. Mills, E. O. Shaffer II and P. H. Townsend, *Adv. Mater.*, 2000, **12**, 1769.
3. The International Technology Roadmap For Semiconductors (ITRS), 2011 Edition
4. P. van der voort, D. Esquivel, E. de Canck, F. Goethals, I. van Driessche and F. J. Romero-Salguero, *Chem. Soc. Rev.*, 2012.
5. Z. L. S. Li, D. Medina, C. Lew, and Y. Yan, *Chem. Mater.*, 2005, **17**, 1851.
6. F. Goethals, I. Ciofi, O. Madia, K. Vanstreels, M. R. Baklanov, C. Detavernier, P. van der voort and I. van Driessche, *J. Mater. Chem.*, 2012, **22**, 8281.
7. H. Y. Yanjun Ma, J. Guo, C. Sathe, A. Agui, and J. Nordgren, *Appl. Phys. Lett.*, 1998, **72**, 3353.
8. M. R. Vengatesan, S. Devaraju, K. Dinakaran and M. Alagar, *J. Mater. Chem.*, 2012, **22**, 7559.
9. H. C. Liu, W. C. Su and Y. L. Liu, *J. Mater. Chem.*, 2011, **21**, 7182.
10. T. Fukumaru, T. Fujigaya and N. Nakashima, *Polym. Chem.*, 2012, **3**, 369.
11. P. Sgarbossa, R. Bertani, V. Di Noto, M. Piga, G. A. Giffin, G. Terraneo, T. Pilati, P. Metrangolo and G. Resnati, *Cryst. Growth Des.*, 2012, **12**, 297.
12. M. Morgen, E. T. Ryan, J. H. Zhao, C. Hu, T. Cho, and P. S. Ho, *Annu. Rev. Mater. Sci.*, 2000, **30**, 645.
13. H. C. Zhou, J. R. Long and O. M. Yaghi, *Chem. Rev.*, 2012, **112**, 673.
14. J. R. Long and O. M. Yaghi, *Chem. Soc. Rev.*, 2009, **38**, 1213.
15. T. T. Luo, H. C. Wu, Y. C. Jao, S. M. Huang, T. W. Tseng, Y. S. Wen, G. H. Lee, S. M. Peng and K. L. Lu, *Angew. Chem., Int. Ed.*, 2009, **48**, 9461.
16. H. L. Tsai, S. L. Yang, Y. H. Liu, R. D. Yadav, C. C. Su, C. H. Ueng, L. G. Lin and K. L. Lu, *Angew. Chem., Int. Ed.*, 2005, **44**, 6063.
17. H. Li, M. Eddaoudi, M. O'Keeffe, and O. M. Yaghi, *Nature*, 1999, **402**, 276.
18. G. Férey, *Chem. Soc. Rev.*, 2008, **37**, 191.
19. S. Kitagawa, R. Kitaura and S. Noro, *Angew. Chem., Int. Ed.*, 2004, **43**, 2334.
20. O. K. Farha, I. Eryazici, N. C. Jeong, B. G. Hauser, C. E. Wilmer, A. A. Sarjeant, R. Q. Snurr, S. T. Nguyen, A. O. Yazaydin and J. T. Hupp, *J. Am. Chem. Soc.*, 2012, **134**, 15016.
21. S. S. Han, J. L. Mendoza-Cortes and W. A. Goddard, *Chem. Soc. Rev.*, 2009, **38**, 1460.
22. L. J. Murray, M. Dinca and J. R. Long, *Chem. Soc. Rev.*, 2009, **38**, 1294.
23. R. E. Morris and P. S. Wheatley, *Angew. Chem., Int. Ed.*, 2008, **47**, 4966.
24. B. Chen, N. W. Ockwig, A. R. Millward, D. S. Contreras and O. M. Yaghi, *Angew. Chem., Int. Ed.*, 2005, **44**, 4745.
25. A. R. Millward and O. M. Yaghi, *J. Am. Chem. Soc.*, 2005, **127**, 17998.
26. L. E. Kreno, K. Leong, O. K. Farha, M. Allendorf, R. P. Van Duyne and J. T. Hupp, *Chem. Rev.*, 2012, **112**, 1105.
27. J. R. Li, R. J. Kuppler and H. C. Zhou, *Chem. Soc. Rev.*, 2009, **38**, 1477.
28. T. Borjigin, F. Sun, J. Zhang, K. Cai, H. Ren and G. Zhu, *Chem. Commun.*, 2012, **48**, 7613.
29. J. Lee, O. K. Farha, J. Roberts, K. A. Scheidt, S. T. Nguyen and J. T. Hupp, *Chem. Soc. Rev.*, 2009, **38**, 1450.
30. L. Ma, C. Abney and W. Lin, *Chem. Soc. Rev.*, 2009, **38**, 1248.
31. D. Farrusseng, S. Aguado and C. Pinel, *Angew. Chem., Int. Ed.*, 2009, **48**, 7502.
32. F. Song, T. Zhang, C. Wang and W. Lin, *Proc. Math. Phys. Eng. Sci.*, 2012, **468**, 2035.
33. C. Y. Sun, C. Qin, C. G. Wang, Z. M. Su, S. Wang, X. L. Wang, G. S. Yang, K. Z. Shao, Y. Q. Lan and E. B. Wang, *Adv. Mater.*, 2011, **23**, 5629.
34. R. C. Huxford, J. Della Rocca and W. Lin, *Curr. Opin. Chem. Biol.*, 2010, **14**, 262.
35. M. D. Allendorf, A. Schwartzberg, V. Stavila and A. A. Talin, *Chemistry*, 2011, **17**, 11372.
36. L. Shen, S. W. Yang, S. Xiang, T. Liu, B. Zhao, M. F. Ng, J. Goettlicher, J. Yi, S. Li, L. Wang, J. Ding, B. Chen, S. H. Wei and Y. P. Feng, *J. Am. Chem. Soc.*, 2012, **134**, 17286.
37. G. C. Xu, W. Zhang, X. M. Ma, Y. H. Chen, L. Zhang, H. L. Cai, Z. M. Wang, R. G. Xiong and S. Gao, *J. Am. Chem. Soc.*, 2011, **133**, 14948.
38. C. I. Yang, P. H. Chuang, G. H. Lee, S. M. Peng and K. L. Lu, *Inorg. Chem.*, 2012, **51**, 757.
39. M. D. Allendorf, C. A. Bauer, R. K. Bhakta and R. J. Houk, *Chem. Soc. Rev.*, 2009, **38**, 1330.
40. T. W. Tseng, T. T. Luo, S. Y. Chen, C. C. Su, K. M. Chi and K. L. Lu, *Cryst. Growth Des.*, 2013, **13**, 510.
41. E. Pardo, C. Train, G. Gontard, K. Boubekeur, O. Fabelo, H. Liu, B. Dkhil, F. Lloret, K. Nakagawa, H. Tokoro, S. Ohkoshi and M. Verdguer, *J. Am. Chem. Soc.*, 2011, **133**, 15328.
42. C. Pan, J. Nan, X. Dong, X. M. Ren and W. Jin, *J. Am. Chem. Soc.*, 2011, **133**, 12330.
43. Q. Chen, P. C. Guo, S. P. Zhao, J. L. Liu and X. M. Ren, *Cryst. Eng. Comm.*, 2013, **15**, 1264.
44. K. Zagorodny, G. Seifert and H. Hermann, *Appl. Phys. Lett.*, 2010, **97**, 251905.
45. S. Eslava, L. Zhang, S. Esconjauregui, J. Yang, K. Vanstreels, M. R. Baklanov and E. Saiz, *Chem. Mater.*, 2013, **25**, 27.
46. P. Reunchan, S. Ouyang, N. Umezawa, H. Xu, Y. Zhang and J. Ye, *J. Mater. Chem. A*, 2013, **1**, 4221.
47. A. D. Aljaberi and J. T. S. Irvine, *J. Mater. Chem. A*, 2013, **1**, 5868.
48. Crystal structure data for **1**: C₁₆H₁₄O₁₁Sr₂ {[Sr₂(1,3-bdc)₂(H₂O)₂·H₂O]_n, M_r = 557.51, monoclinic, C2/c, a = 24.074(5) Å, b = 12.735(3) Å, c = 13.455(3) Å, β = 118.63(3)°, V = 3620.5(12) Å³, Z = 8, ρ_{calcd} = 2.046 g/cm³, μ = 5.955 mm⁻¹, λ (Mo Kα) = 0.7107 Å, F(000) = 2192, T = 296(2) K. Final R indices: R₁ = 0.0260, wR_{2a} = 0.0518 [I > 2σ(I)]; R₁ = 0.0388, wR_{2a} = 0.0557 [all data], GOF = 1.026. CCDC = 936413 (**1**) contains the supplementary crystallographic data for this paper. These data can be obtained free of charge from the Cambridge Crystallographic Data Centre via www.ccdc.cam.ac.uk/data_request/cif.
49. H. B. Cui, K. Takahashi, Y. Okano, H. Kobayashi, Z. Wang and A. Kobayashi, *Angew. Chem., Int. Ed.*, 2005, **44**, 6508.
50. B. Zhou, A. Kobayashi, H. B. Cui, L. S. Long, H. Fujimori and H. Kobayashi, *J. Am. Chem. Soc.*, 2011, **133**, 5736.
51. D. R. Patil, S. A. Lokare, R. S. Devan, S. S. Chougule, C. M. Kanamadi, Y. D. Kolekar and B. K. Chougule, *Mater. Chem. and Phys.*, 2007, **104**, 254.
52. Y. Z. Tang, X. F. Huang, Y. M. Song, P. W. Hong Chan and R. G. Xiong, *Inorg. Chem.*, 2006, **45**, 4868.
53. C. C. Homes, T. Vogt, S. M. Shapiro, S. Wakimoto and A. P. Ramirez, *Science*, 2001, **293**, 673.
54. H. X. Zhao, J. X. Liu, L. S. Long, A. A. Bokov, Z. G. Ye, R. B. Huang and L. S. Zheng, *J. Phys. Chem. C*, 2012, **116**, 14199.
55. D. W. Fu, H. Y. Ye, Q. Ye, K. J. Pan and R. G. Xiong, *Dalton Trans.*, 2008, 874.
56. D. C. Sinclair, T. B. Adams, F. D. Morrison and A. R. West, *Appl. Phys. Lett.*, 2002, **80**, 2153.
57. M. Sánchez-Andújar, S. Yáñez-Vilar, B. Pato-Doldán, C. Gómez-Aguirre, S. Castro-García and M. A. Señarís-Rodríguez, *J. Phys. Chem. C*, 2012, **116**, 13026.
58. B. Pato-Doldán, M. Sanchez-Andujar, L. C. Gomez-Aguirre, S. Yanez-Vilar, J. Lopez-Beceiro, C. Gracia-Fernandez, A. A. Haghghirad, F. Ritter, S. Castro-Garcia and M. A. Senaris-Rodriguez, *Phys. Chem. Chem. Phys.*, 2012, **14**, 8498.

Cite this: DOI: 10.1039/c0xx00000x

www.rsc.org/xxxxxx

ARTICLE TYPE

Table of Contents

A strontium-based metal–organic framework exhibits intrinsic low dielectric constant (k) after removing the water molecules. A low dielectric constant and high thermal stability make this compound a candidate for use as a low- k material for potential interlayer dielectric applications.

5

